

Growth and ultrastructure of *Arabidopsis* root hairs: the *rhd3* mutation alters vacuole enlargement and tip growth

M.E. Galway^{1,*}, J.W. Heckman, Jr.², J.W. Schiefelbein¹

¹ Department of Biology, The University of Michigan, Ann Arbor, MI 48109-1048, USA

² Center for Electron Optics, Michigan State University, East Lansing, MI 48824-1311, USA

Received: 21 May 1996/Accepted: 29 June 1996

Abstract. The root hairs of plants are tubular projections of root epidermal cells and are suitable for investigating the control of cellular morphogenesis. In wild-type *Arabidopsis thaliana* (L.) Heynh, growing root hairs were found to exhibit cellular expansion limited to the apical end of the cell, a polarized distribution of organelles in the cytoplasm, and vesicles of several types located near the growing tip. The *rhd3* mutant produces short and wavy root hairs with an average volume less than one-third of the wild-type hairs, indicating abnormal cell expansion. The mutant hairs display a striking reduction in vacuole size and a corresponding increase in the relative proportion of cytoplasm throughout hair development. Bead-labeling experiments and ultrastructural analyses indicate that the wavy-hair phenotype of the mutant is caused by asymmetric tip growth, possibly due to abnormally distributed vesicles in cortical areas flanking the hair tips. It is suggested that a major effect of the *rhd3* mutation is to inhibit vacuole enlargement which normally accompanies root hair cell expansion.

Key words: *Arabidopsis* (mutant, root hairs) – Mutant (*Arabidopsis rhd3*) – Root hair (ultrastructure) – Tip growth – Vacuole

Introduction

Root hairs are tubular outgrowths formed by epidermal cells in the roots of plants. The hairs elongate away from the root surface by growth restricted to their tips. This mode of cell expansion, known as tip growth, occurs in a variety of often dissimilar cell types such as pollen tubes and root hairs in plants, fungal hyphae and moss protonemata (Sievers and Schnepf 1981; Schnepf 1986). In

tip-growing cells, new plasma membrane and cell wall components are incorporated continuously into the growing tips by polarized exocytosis.

The rapid and localized growth of root hairs make them a favorable cell type with which to study cell morphogenesis in plants. Using rapid freezing and freeze-substitution methods, general ultrastructural features of growing root hairs have been identified in several different plant species (Ridge 1988; Derksen and Emons 1990; Ridge 1996). The extreme tips of growing root hairs are filled with large numbers of secretory vesicles containing cell wall components (Sherrier and VandenBosch 1994). The presence of secretory vesicles is correlated with growth, for when tip growth slows or stops, secretory vesicles disappear (Sievers and Schnepf 1981; Derksen and Emons 1990). Organelles and other cell structures involved in the biosynthesis and transport of macromolecules are concentrated in the subapical region, a cytoplasmic region just behind the extreme tips of the hairs. Behind the cytoplasmic regions, growing root hairs are filled with large central vacuoles, which enlarge in concert with the expansion of the cell.

Arabidopsis thaliana has been the subject of several recent studies of root hair growth and development, due to its small size and the ease with which molecular genetic analyses can be conducted with this plant (Schiefelbein and Somerville 1990; Schiefelbein et al. 1992; Dolan et al. 1994; Bates and Lynch 1996). The isolation and initial characterization of a collection of root hair morphology mutants of *Arabidopsis* has been described (Schiefelbein and Somerville 1990). One of these mutants, *rhd3*, produces short roots and root hairs that are short and wavy, implying that the *RHD3* gene normally is required for regulated cell expansion (Schiefelbein and Somerville 1990). In the present study, we have analyzed the growth and ultrastructure of wild-type root hairs of *Arabidopsis*, in order to provide a foundation for future studies of root hair development in this plant. We have also analyzed root hair formation in the *rhd3* mutant, and we find that the mutant hairs differ in vacuole enlargement and in vesicle distribution during root hair growth.

* Present address: Department of Biology, St. Francis Xavier University, Antigonish, Nova Scotia, B2G 2W5, Canada

Correspondence to: J.W. Schiefelbein; Tel: 1 (313) 764 3580; FAX: 1 (313) 747 0884; E-mail: schiefel@umich.edu

Materials and methods

Plant material and seedling growth. The *rhd3* allele used in this study (*rhd3-1*) possesses the most severe mutation affecting the *RHD3* gene and was generated by ethyl methanesulfonate mutagenesis of wild-type (Columbia) *Arabidopsis thaliana* seeds (L.) Heynh. (Schiefelbein and Somerville 1990). Seedlings were grown in sealed, vertically-oriented Petri plates on media (designated AMM) as previously described (Schiefelbein and Somerville 1990). Seedlings grown on agarose (Gibco-BRL)-solidified medium produce consistently longer roots and root hairs than seedlings grown on agar (Difco Bacto-Agar)-solidified media (data not shown), and this probably accounts for differences in *rhd3* root hair length reported here and in an earlier paper (Schiefelbein and Somerville 1990).

Measurements and light microscopy of root hairs. Root-hair length was determined from 100 hairs from the upper half of 20 roots of 5- to 6-d-old seedlings. Root hair diameter was determined from the center portion of 20 hairs of 5-d-old seedlings. The cytoplasm of living root hairs was observed by staining seedlings in a 0.005% solution of fluorescein diacetate (Sigma Chemical, St. Louis, Mo., USA).

Microbead labeling of hairs to monitor growth. To monitor hair growth, 4- or 5-d-old seedlings were placed inside observation chambers constructed according to Heath (1985). Growing hairs were labeled with polylysine-coated beads (0.5 μm in diameter), according to Staebell and Soll (1985). The rate of root hair elongation and the length of the apical expansion zone were determined from micrographs taken at timed intervals after the bead labeling.

Cryofixation and freeze substitution. The roots of 5- to 6-d-old seedlings were excised at the hypocotyls, held in fine forceps at the cut end and rapidly frozen by plunging into a 40-ml aluminum reservoir filled with liquid propane (for details, see Galway et al. 1995). The roots were freeze-substituted in 1% OsO_4 in acetone for 3 d at -80°C before rewarming over an 8- to 12-h-period in an insulated storage box. As soon as the substitution solution reached 0°C , the samples were given three changes of electron-microscope-grade anhydrous acetone to remove any unreacted OsO_4 , and allowed to warm to room temperature. The roots were then infiltrated through a graded resin series and embedded, using either Spurr's resin (Spurr 1969) or a Quetol/VCD-based resin formulation (Kushida 1974) for sectioning and transmission electron microscopy.

Electron microscopy. Ultra-thin sections of root hairs were cut on a diamond knife, mounted on Formvar-coated, 50-mesh copper Gilder grids (Ted Pella Inc., Redding, Cal., USA), stained in aqueous 2% uranyl acetate followed by lead citrate (Reynolds 1963), and viewed in a 300 model Philips electron microscope operating at 60 kV. Sections of 29 cryofixed root hairs from 7 different wild-type seedling roots and 16 hairs from 7 different *rhd3* seedling roots were examined. The distribution of secretory vesicles was determined by comparing the vesicle number in each of nine pie-shaped segments from transverse hair sections ($n = 7$) taken between 1 μm and 3 μm from the hair tip (prior to vacuole formation).

Results

Analysis of wild-type and mutant root hairs by light microscopy

Three regions could be distinguished along the length of seedling roots of *Arabidopsis thaliana* (Fig. 1A, E). In the first region, within approximately 1 mm of the root apex, no root hairs were present on the root surface; this region

contained trichoblasts (root hair cell precursors). Elongating hairs (growing hairs) were located in a second region of the root (approximately 1–2 mm from the apex). The third region were composed of non-elongating hairs (mature hairs) which cover the remainder of the root (Fig. 1A, E).

At the time of root hair initiation, the wild-type trichoblasts were approximately 190 μm long (Table 1), and they were extensively vacuolated. As a root hair emerged, near the apical end of the elongated cell, the nucleus migrated from a position in the middle of the trichoblast (Fig. 2B) toward the site of the emerging hair (Fig. 2F), and it eventually entered the growing hair.

In growing root hairs of the wild type, a zone of cytoplasm filled the hair tip and extended about 60–80 μm behind the tips (Fig. 2F). Below the cytoplasmic tips, the hairs were highly vacuolated. When fully developed, the hairs had an average length of 0.8 mm and an average diameter of 11 μm (Table 1). These hairs grew at an average rate of 1.3 $\mu\text{m}/\text{min}$ (Table 1), which is similar to the late growth rate of *Arabidopsis* root hairs reported in previous studies (Schiefelbein et al. 1992; Dolan et al. 1994; Bates and Lynch 1996). All wild-type hairs contained large centrally-located vacuoles, with cytoplasm present in a thin layer at the periphery (cortex) of the hairs (Fig. 1C, D). The tip cytoplasm that was present in growing hairs was not found in the tips of mature wild-type hairs.

Analysis of the *rhd3* mutant root hairs revealed several differences compared to the wild type (Figs. 1, 2). At the onset of root hair formation, trichoblasts in *rhd3* seedling roots were significantly shorter (less than one-half wild-type length; Table 1) and contained smaller vacuoles than wild-type trichoblasts (not shown). The developing *rhd3* cells were similar to the wild type in the position and migration of nuclei, and, like the wild type, *rhd3* hairs emerged at the apical ends of the trichoblasts (Fig. 2A, G). Mature *rhd3* hairs were shorter than the wild type and often exhibited a subtle wavy shape (Fig. 1F–H), with irregular curvatures along the length of the hair. The average length of mature *rhd3* hairs was 0.19 mm (24% of wild type) and their average diameter was not significantly different from that of wild type hairs (Table 1). Thus, the volume of the *rhd3* mutant hairs averaged less than one-third of the volume of the wild-type root hairs. This was associated with a reduction in the rate of root hair elongation (0.6 $\mu\text{m}/\text{min}$) in the *rhd3* mutant (Table 1).

The reduction in cell volume was associated with a relative increase in the proportion of cytoplasm in the *rhd3* hairs. Large vacuoles were present shortly after the emergence of wild-type hairs, but not *rhd3* hairs (compare Fig. 2E, F and 2H, I). In mature hairs, the *rhd3* mutant lacked tip cytoplasm, like the wild type, but possessed a relatively large amount of cytoplasm throughout the rest of the hair (compare Fig. 1D and 1H). This excess cytoplasm took the form of large masses or strands of cytoplasm that extended between the base and the hair tip (Fig. 1G, H). These strands were first observed when the bases of growing hairs became vacuolated, and they extended along the basal side of the hair and into the epidermal cell proper (Fig. 2A). These results indicate that the *rhd3* mutation alters the relative proportion of cytoplasm and vacuole throughout root hair cell expansion.

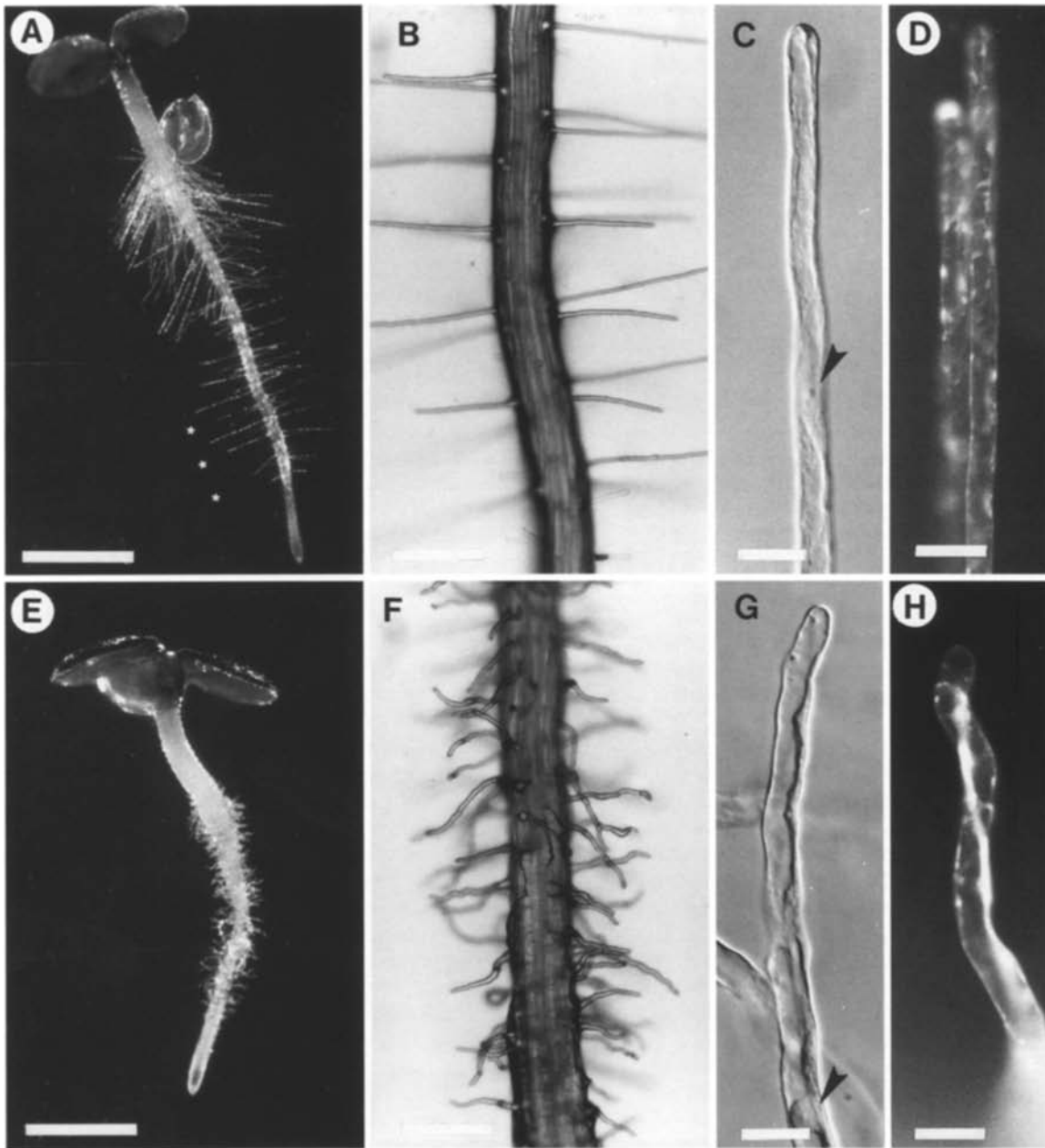


Fig. 1A–H. Root hairs of *Arabidopsis thaliana*. **A–D** Wild type (Columbia); **E–H** *rhd3* mutant. **A, E** Five-day-old seedlings, with the *rhd3* seedlings (**E**) bearing shorter root hairs compared to the wild type (**A**). File of asterisks in **A** indicates the zone of growing and elongating hairs. $\times 8$; bars = 2 mm. **B, F** Root hairs along a wild-type (**B**) and *rhd3* (**F**) root; note the short and wavy *rhd3* hairs. $\times 65$; bars = 200 μm . **C, G** Mature root hairs of the wild type (**C**) and *rhd3* (**G**) visualized by differential interference contrast optics. Nuclei (arrowheads) are visible in both hairs. $\times 500$; bars = 20 μm . **D, H** Fluorescein diacetate stains the cortical cytoplasm in a mature wild-type hair (**D**) and stains a large, axially-oriented cytoplasmic strand in a mature *rhd3* hair (**H**). $\times 500$; bars = 20 μm

Monitoring root hair growth by microbead labeling

When growing root hairs were exposed to polylysine-coated beads, the beads adhered firmly to the hairs on contact. Hairs continued to grow regardless of the number or position of beads on their surfaces, and thus, the relative position of the beads at various times after initial attachment could be determined. In 22 wild-type and *rhd3* hairs labeled with beads, the distance between the at-

tached beads and the tip of each hair increased as hair growth continued, whereas the distance between the attached beads and the base of each root hair remained fixed (see Fig. 2B–F, 2G–L). This result showed that, as expected, cell expansion in *Arabidopsis* root hairs is restricted to the tip. Furthermore, by measuring the distance between pairs of beads in timed micrographs, the zone of hair expansion was determined to extend $4.3 \pm 1.0 \mu\text{m}$ and $6.0 \pm 3.4 \mu\text{m}$ from the apex in the wild-type and *rhd3*

Table 1. Trichoblast and root hair characteristics in wild-type and mutant *Arabidopsis* seedlings^a

Genotype	Trichoblast length (mm)	Root hair length (mm)	Root hair diameter (μm)	Root hair growth rate ($\mu\text{m}/\text{min}$)
Columbia wild type	0.19 \pm 0.04	0.8 \pm 0.2	11 \pm 2	1.3 \pm 0.3
<i>rhd3</i> mutant	0.08 \pm 0.02	0.19 \pm 0.05	13 \pm 4	0.6 \pm 0.2

^a Values indicate the mean \pm SD

mutant hairs, respectively. The increased variation in the length of the *rhd3* expansion zone indicates that the *rhd3* mutation may alter the spatial control of apical hair expansion.

In these developmental time course experiments, growing root hairs of *rhd3* mutants (but not wild-type hairs) exhibited irregular changes in the direction of expansion at their tips. Figure 2G–L illustrates one such growing hair as it was observed over a 55-min period. These observations indicate that the wavy-hair phenotype of the *rhd3* mutant is due to irregular changes in the direction of root hair growth associated with differential expansion about the root hair tip.

Ultrastructure of wild-type and *rhd3* mutant root hairs

Optimal preservation of root hair ultrastructure was obtained by fixing seedling roots by a rapid freezing and freeze-substitution method (Emons 1987; Ridge 1988; Sherrier and VandenBosch 1994; see *Materials and methods*). In these hairs (Figs. 3–6), the plasma membrane was appressed to the cell wall, and membranes surrounding organelles and vacuoles were smooth and taut. Secretory vesicles in the tips of growing hairs retained darkly-stained contents after cryofixation, although cellular membranes were usually not positively stained by the uranyl acetate/lead citrate method after cryofixation; occasionally cell walls also failed to stain well (e.g. Fig. 3).

Electron microscopy of near-median longitudinal sections at the tip of growing wild-type and *rhd3* mutant root hairs revealed a characteristic polarized distribution of organelles and cytoplasm (Fig. 3A, B). A region of cytoplasm at the extreme apex of each hair contained large numbers of secretory vesicles. Below this lay an organelle-rich subapical region containing large numbers of Golgi bodies and mitochondria as well as some multivesicular bodies. An area of smooth and ribosome-coated endoplasmic reticulum was located between the apical and subapical regions. Vacuoles occupied the majority of the basal regions of the wild-type and mutant hairs, with plastids often located in the cytoplasm of the vacuolated regions.

Vesicles and the cytoskeleton in growing hairs. At the tip of growing wild-type and mutant hairs, densely staining secretory vesicles were abundant and possessed spherical or pleiomorphic shapes (Fig. 4). Some pleiomorphic vesicles were elongated, some were tear-drop shaped, and others bore thin tube-like projections. In addition, coated pits were observed on the plasma membrane along with coated vesicles near the plasma membrane (Fig. 4A, B).

Coated vesicles (exclusive of their coats) were smaller than most secretory vesicles (which ranged from 60 to 100 nm in diameter).

Series of transverse sections from the apical and subapical regions of growing wild-type and *rhd3* hairs revealed differences in secretory vesicle distribution (Fig. 5). In *rhd3* hairs, abnormally large numbers of secretory vesicles were concentrated in localized areas of the subapical regions (Fig. 5B–D). In wild-type hairs, large numbers of densely packed secretory vesicles were observed only in the apical regions of hairs (Fig. 5E); secretory vesicles were sparse and scattered in the organelle-rich subapical and vacuolated regions of the hairs (Fig. 5F). Comparison of secretory vesicle distribution in sections of wild-type and mutant hairs revealed a statistically significant deviation from a random distribution in the subapical sections of the *rhd3* mutant ($P < 0.001$). These observations indicate that the abnormal tip growth in the *rhd3* mutant hairs is associated with an asymmetric distribution of secretory vesicles.

The microfilament and microtubule organization in growing root hairs of the wild-type and *rhd3* mutant were not significantly different. Microfilaments were detected among the secretory vesicles in the apical regions of growing wild-type and mutant hairs, but these were not well preserved. In the subapical and vacuolated regions, microfilaments formed prominent bundles or cables oriented parallel to the long axes of the hairs. Secretory vesicles and organelles were often aligned along such bundles (Fig. 4D). Most microtubules in wild-type and mutant hairs lay just under the plasma membrane (cortical microtubules), and were oriented parallel to the long axes of the hairs (Fig. 6). Axially oriented endoplasmic microtubules were abundant in *rhd3* hairs, and often lay close to the vacuoles (Fig. 6C–E).

Vacuoles in growing and mature hairs. Large, centrally positioned vacuoles filled the basal regions of growing wild-type hairs, with smaller vacuoles or finger-like extensions of the larger basal vacuoles present between the subapical and basal regions. In the growing hairs of the *rhd3* mutant, the area occupied by vacuoles was smaller than in the wild-type hairs (for example, compare Fig. 6A and B).

In mature hairs of the wild type, a thin layer of peripheral cytoplasm and no secretory vesicles were observed near the tip (Fig. 3C). These mature hairs were extensively vacuolated throughout their length, characterized by a large central vacuole containing particulate material (Fig. 3C). In contrast, mature *rhd3* hairs contained a thicker layer of peripheral cytoplasm and a smaller

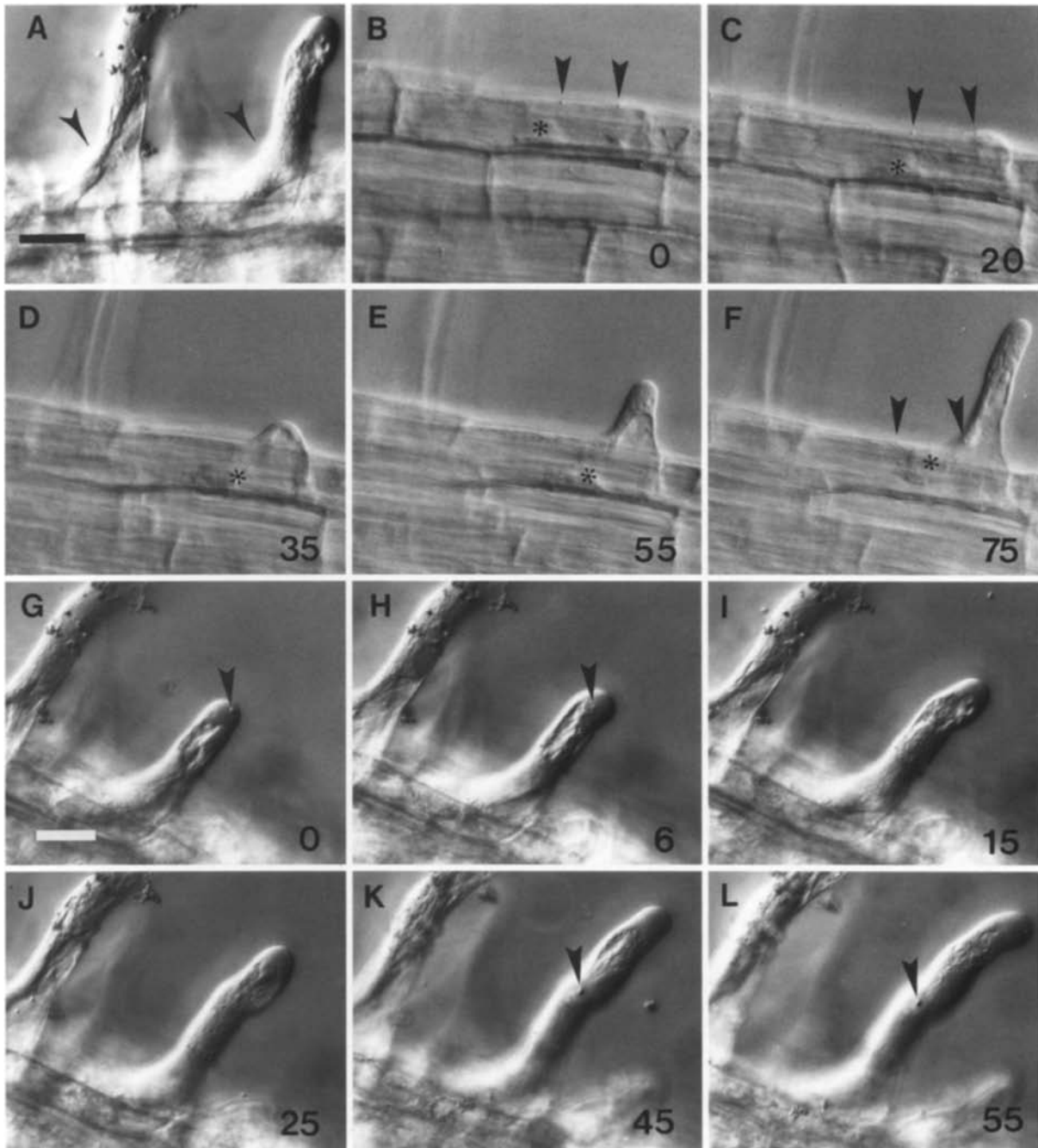


Fig. 2A–L. Growth and development of wild type (**B–F**) and *rhd3* (**A, G–L**) root hairs. **A** Developing *rhd3* root hairs contain axial cytoplasmic strands. The hair on the right is younger and exhibits a larger amount of cytoplasm in connection with the epidermal cell proper (*arrowheads*), compared to the more developmentally-advanced hair on the left. **B–L** Developmental time-course study of root hair growth in 4-d-old wild-type (**B–F**) or *rhd3* (**G–L**) seedling roots labelled with microbeads (*arrowheads*). Time is given in minutes from the start of observation (at the lower right of each micrograph). Bead visibility in each micrograph is dependent on the plane of focus. In panels **B–F**, the position of the nucleus is indicated by *asterisks*. All panels are at same magnification: $\times 465$; bar in panel **A** = 20 μm

central vacuole. This was particularly evident in electron micrographs of sections obtained within 1 μm of the hair tips (Fig. 3D). Sections obtained from 1 to 5 μm from the *rhd3* tips revealed successively larger central vacuoles, and a smaller layer of cytoplasm, yet the relative amount of cytoplasm was consistently greater than in the wild-type

mature hairs (not shown). The mutant hairs also exhibited an unusually wavy plasma membrane, even though the cell walls were closely appressed to the plasma membrane (Fig. 3D). These findings show that the *rhd3* hairs exhibit abnormalities in the amount of cytoplasm relative to vacuole throughout their development.

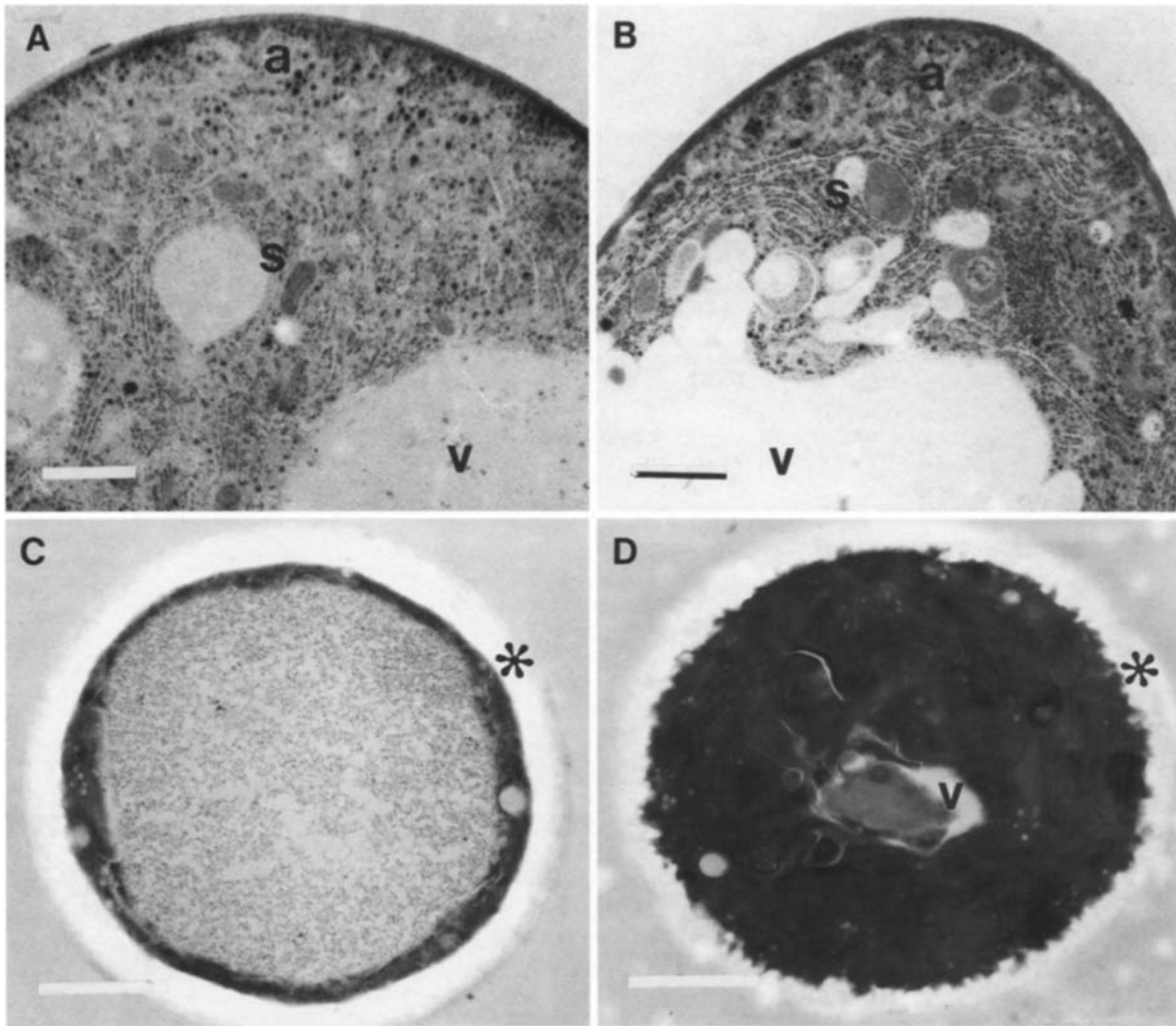


Fig. 3A–D. Ultrastructure of growing (A, B) and mature (C, D) *Arabidopsis* root hairs. A, B. Near-median sections of growing wild-type (A) and *rhd3* (B) root hairs. Both sections possess part of the vesicle-rich apical region (a), the organelle-rich subapical region (s) and the basal vacuolated region (v) characteristic of these hairs. $\times 12\,500$; bars = $1\ \mu\text{m}$. C, D. Transverse sections approximately $1\ \mu\text{m}$ from the tips of mature wild type (C) and *rhd3* (D) root hairs. In each section, cell walls are unstained (asterisks) and cytoplasm is intensely stained. A large vacuole containing particulate material fills the center of the wild-type hair; a much smaller vacuole (v) containing dense material is present in the *rhd3* root hair. Note the wavy plasma membrane in the mature *rhd3* hair. $\times 17\,280$; bars = $1\ \mu\text{m}$

Discussion

Features of root hair development in *Arabidopsis*. In this study, we have analyzed the growth and ultrastructure of root hairs of the wild type and a mutant of *Arabidopsis thaliana*. Many of the features identified in the root hairs of *Arabidopsis* are similar to those reported for other plant species or for other tip-growing cells (Sievers and Schnepf 1981; Schnepf 1986; Ridge 1996). For example, we used bead-labeling studies to demonstrate that root hairs of *Arabidopsis* enlarge by growth restricted to a small region of the tips. Also, a polarized organization of organelles and vesicles was identified at the growing tip of *Arabidopsis* root hairs. In addition, the organization of microtubules and microfilaments in *Arabidopsis* root hairs is similar to that reported for other cryopreserved root hairs (Emons and Traas 1986; Emons 1987; Derksen and

Emons 1990). Furthermore, coated pits and coated vesicles were found near the tips of growing *Arabidopsis* hairs, where they may participate in membrane turnover (Emons and Traas 1986; Ridge 1988; Derksen et al. 1995).

We have identified a variety of vesicle types, including coated vesicles and pleiomorphic vesicles, near the tips of growing *Arabidopsis* root hairs. The coats detected on secretory vesicles in *Arabidopsis* (present study) and on *Vicia* hairs (Ridge 1988) may be required to direct fusion events (Kiss et al. 1990; Derksen et al. 1995). The pleiomorphic vesicles reported here are similar to the pyriform (or pear-shaped) vesicles first reported in *Vicia* root hairs (Ridge 1988; Ridge 1995). These vesicles have not been distinguished here from secretory vesicles because they are found among normal spherical secretory vesicles, they are similar in size, and the staining of vesicle contents is similar. The various vesicle shapes may arise

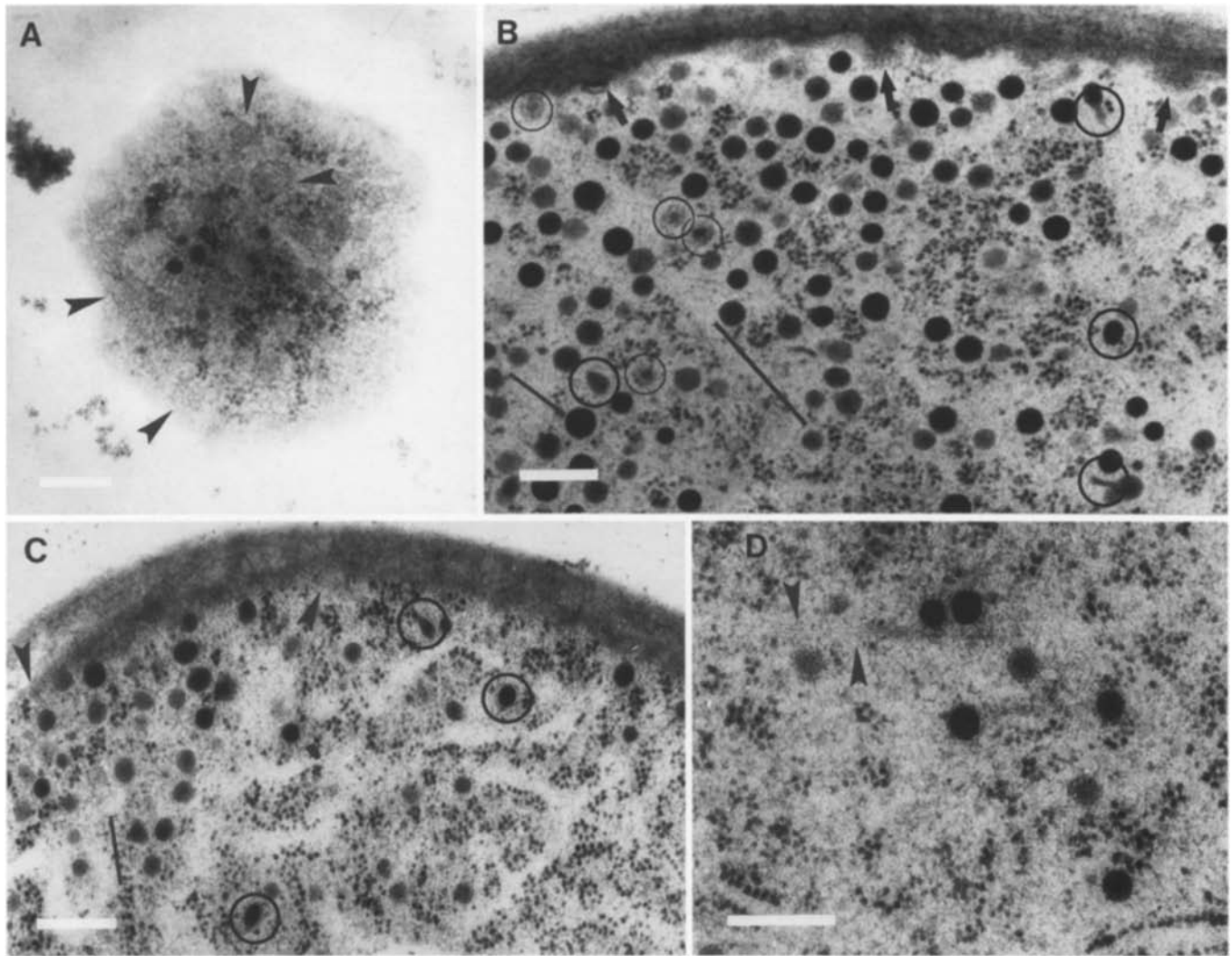


Fig. 4A–D. Vesicles and cytoskeletal components in growing wild type (**A, C, D**) and *rhd3* (**B**) root hairs. **A** A transverse section grazing the plasma membrane and cytoplasm at the extreme tip of a hair. Coated pits (*arrowheads*) are visible along with darkly staining vesicles. $\times 52\,400$; bar = 200 nm. **B** Vesicles near the cell wall in a transverse section of an *rhd3* hair. Note coated vesicles (*small circles*) among the darker secretory vesicles and coated pits (*arrows*) at the plasma membrane. Some secretory vesicles are ovoid or have a tube-like extension (*large circles*). Some microfilaments are present among the vesicles (along *black bars*). $\times 56\,960$; bar = 200 nm. **C** A steep oblique section grazing the apical and subapical regions. Some secretory vesicles are ovoid or teardrop-shaped (*circles*), and many have detectable coats. One vesicle lies adjacent to a microfilament (along *black bar*). Two axially oriented cortical microtubules lie close to the plasma membrane (*arrowheads*). $\times 56\,960$; bar = 200 nm. **D** A group of coated secretory vesicles in the subapical region is aligned along a small bundle of microfilaments (*arrowheads*). $\times 81\,060$; bar = 200 nm

from the action of physical forces, such as vesicle-vesicle interactions or from the attachment of vesicles to other structures such as microfilaments.

Altered root hair development in rhd3 mutants. The major defect associated with the *rhd3* root hairs is a reduction in cell size. On average, the *rhd3* root hairs possess less than one-third of the volume of wild-type hairs. This reduction in hair volume implies that the *rhd3* mutation inhibits root hair cell expansion.

Cell expansion in plants occurs when the cell wall yields to the internal turgor pressure and undergoes irreversible wall extension (Taiz 1984; Cosgrove 1986). Increase in cell volume results from the uptake of water, which accumu-

lates preferentially in the vacuole (Wiebe 1978; Cosgrove 1993). Thus, cell expansion is generally accompanied by vacuole enlargement and a corresponding decrease in the relative proportion of cytoplasm. We have shown that expanding root hair cells in wild-type *Arabidopsis* plants are also associated with extensive vacuole enlargement. However, the *rhd3* mutant root hairs possess smaller vacuoles and a larger proportion of cytoplasm than the wild type at all stages of hair formation, including root-hair precursor cells, growing root hairs, and mature root hairs. The vacuolar abnormalities are specific to the *rhd3* mutant; they are not observed in the wild type when hair growth is inhibited by environmental factors nor are they observed in other root-hair mutants with shortened hairs

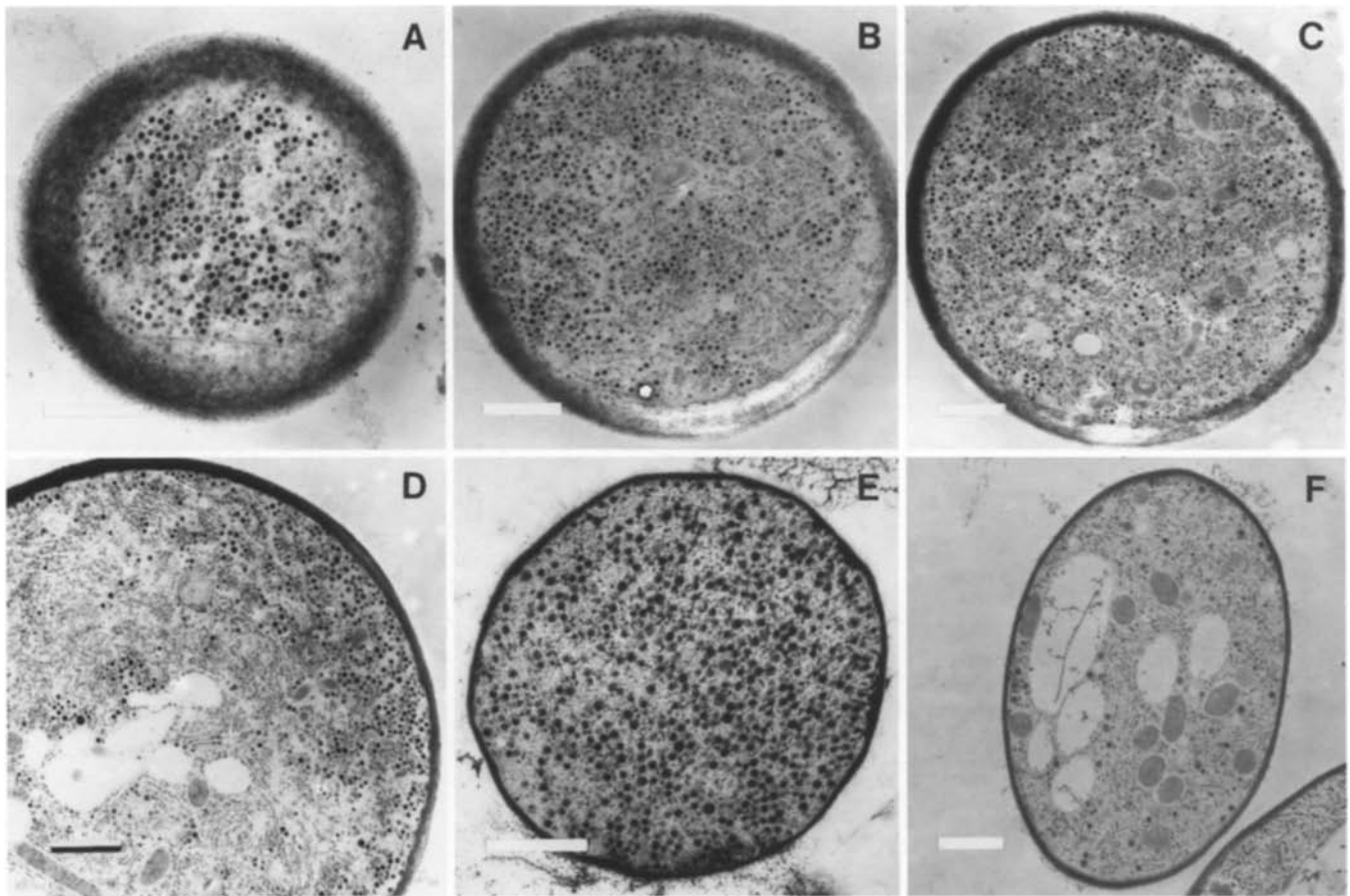


Fig. 5A–F. Secretory vesicle distribution in growing *rhd3* (A–D) and wild-type (E, F) root hairs. A–D Sequential transverse sections from the apical (A) and subapical (B–D) regions of a single *rhd3* hair. Large numbers of secretory vesicles are present, but not uniformly distributed, throughout the subapical region. Bars = 1 μm. A Section approx. 1 μm from the tip, × 13 290; B section approx. 1.5 μm from the tip, × 10 460; C section approx. 2 μm from the tip, × 8550; D section approx. 3 μm from the tip, × 8760. E A section from the apical region, approximately 1.5 μm from the tip, of a wild-type hair showing numerous secretory vesicles (hair has been damaged by ice crystal formation during freeze-fixation process). × 13 290; bar = 1 μm. F Oblique section from the lower subapical region, approximately 3 μm from the tip, of a wild-type hair. Relatively few secretory vesicles are present compared to a similar region of the *rhd3* hair in D. × 8550; bar = 1 μm

(data not shown). Thus, the vacuole defects in *rhd3* are not likely to represent a secondary effect of an inhibition of hair cell expansion. Based on these observations, a major effect of the *rhd3* mutation may be to inhibit vacuole enlargement, which leads to a reduction in hair cell expansion.

The *rhd3* root hairs also exhibit a relatively subtle alteration in cell shape. Time-lapse microscopy experiments showed that the wavy hair morphology is due to occasional deformations of the hemispherical root hair tip and subsequent changes in the direction of cell expansion. In other tip-growing cells, bending is usually due to either differential expansion at the flanks of the tip, or to a complete redirection of tip growth to a subapical, flanking position (Sievers and Schnepf 1981). Since the *rhd3* hairs do not form sharp right-angle bends, differential expansion is the most likely mode of bending in these hairs. Ultrastructural analysis of growing *rhd3* hairs revealed an altered distribution of secretory vesicles, with large numbers of vesicles in localized areas of the subapical regions. Assuming that secretory vesicles fuse close to where they

are concentrated, the skewed distribution of secretory vesicles in the subapical regions could lead to the observed differential growth at the flanks of the hair tips.

The relationship between the vacuolar and cell shape defects in the *rhd3* mutant root hairs is not clear. It is possible that the massive reduction in vacuole enlargement is responsible for the tip growth irregularities. In this regard, it is noteworthy that in Bartnicki-Garcia's mathematical model for the morphogenesis of fungal hyphae (Bartnicki-Garcia 1990; Bartnicki-Garcia et al. 1995), wavy hyphae can be generated by lateral movements in the net forward motion of a hypothetical vesicle supply center (VSC). The VSC is defined as "a site from which vesicles start on the final leg of their journey to the cell surface" (Bartnicki-Garcia 1990). If this model is applied to the wild-type *Arabidopsis* hair, the continual expansion of the central vacuole in growing hairs could provide a uniform force to advance the VSC tipwards, as required by the model in order to generate a tubular cell. The abnormal arrangement of cytoplasm and vacuoles in *rhd3* hairs might then lead to lateral oscillations of a VSC,

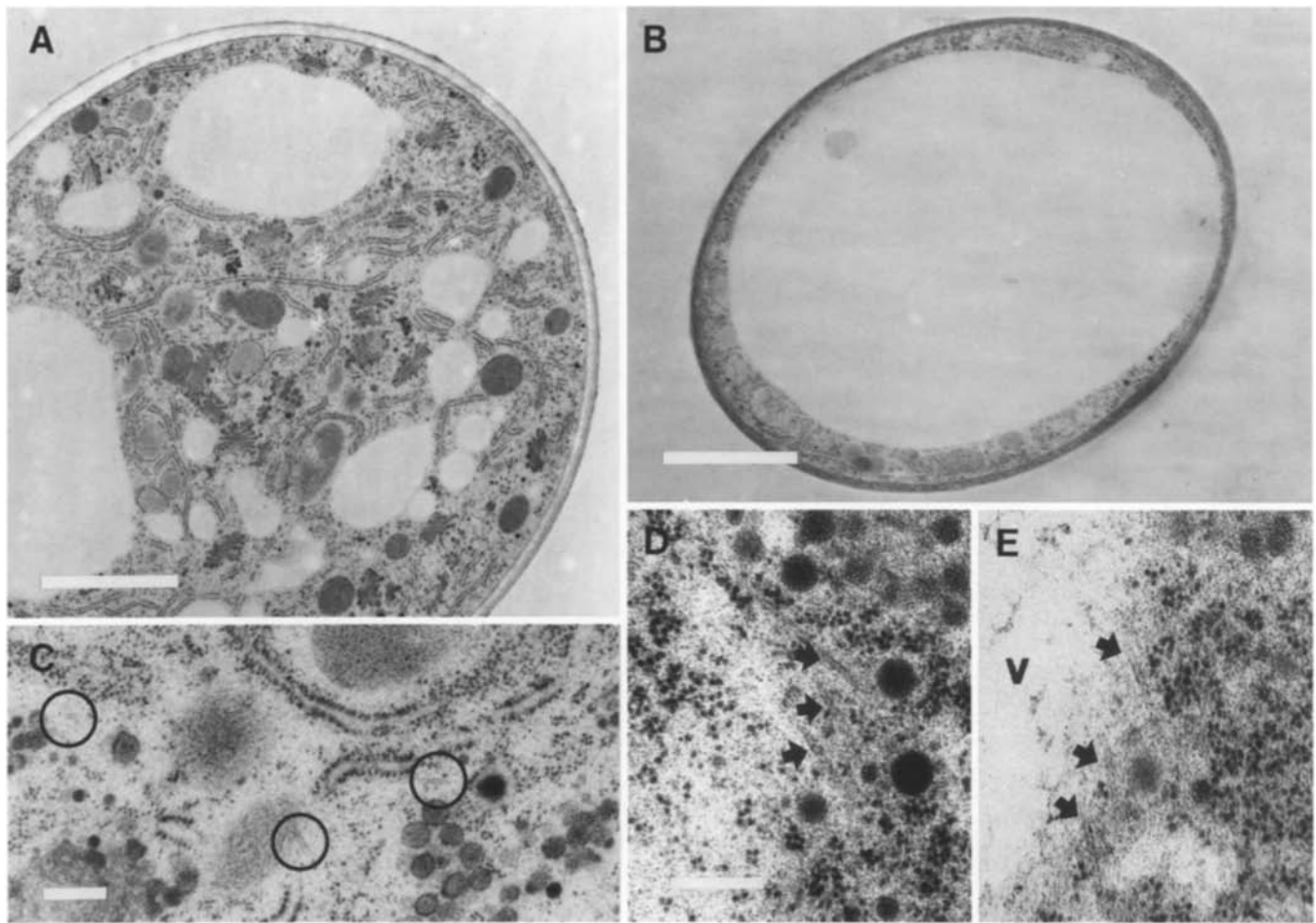


Fig. 6A–E. Cytoplasm and vacuoles in growing root hairs of *rhd3* (A, C, D, E) and wild-type (B) plants. A, B Several large vacuoles are present in the transverse section from the vacuolated region of a growing *rhd3* hair (A; $\times 8760$; bar = 2 μm) rather than the single large central vacuole characteristic of growing wild-type hairs (B; $\times 8550$; bar = 2 μm). The wild-type section (B) comes from a more apical part of the hair (approx. 5 μm from the tip) than does the *rhd3* hair section (approx. 6–8 μm from the tip), yet it still possesses a much larger vacuole than the *rhd3* section. C Endoplasmic microtubules (circles) are present in this detail from the center of the hair in (A). $\times 39\,740$; bar = 200 nm. D, E A group of microtubules (arrows) viewed in two different sections from the subapical region (D) and the upper part of the vacuolated region (E) of an *rhd3* hair. The microtubules are aligned near the surface of a large vacuole (V). $\times 58\,320$; bar = 200 nm

which could result in changes in the direction of root hair growth.

At present, the molecular basis for the reduced vacuole size in the *rhd3* mutant root hairs is unknown. One possibility is that the *RHD3* gene product may normally participate directly in vacuole biogenesis. Vacuoles appear to arise/enlarge by incorporation of membranes derived from the endoplasmic reticulum (Boller and Wiemken 1986); perhaps the *rhd3* mutation alters the accumulation or turnover of vacuolar membranes or their component proteins. Another possibility is that the *RHD3* gene product may normally regulate solute fluxes during cell expansion. The vacuole accumulates solutes as it enlarges (Boller and Wiemken 1986; Cosgrove 1986; Cosgrove 1993); if the *rhd3* mutation inhibits solute acquisition, water uptake (and cell expansion) would be reduced. Analysis of expansion in other cells of the *rhd3* mutant and the molecular isolation of the *RHD3* gene will be required to define the biochemical nature of the vacuolar defect.

We thank Celeste Malinoski, David Bay, and Shelley Almburg for technical assistance. This research was supported by National Science Foundation grants IBN-9316409 and IBN-9258223 to J.W.S., and a National Sciences and Engineering Research Council of Canada postdoctoral award to M.E.G.

References

- Bartnicki-Garcia S (1990) Role of vesicles in apical growth and a new mathematical model of hyphal morphogenesis. In: Heath IB (ed) Tip growth in plant and fungal cells. Academic Press, San Diego, pp 211–232
- Bartnicki-Garcia S, Bartnicki DD, Gierz G (1995) Determinants of fungal cell wall morphology: the vesicle supply center. *Can J Bot* (Suppl. 1): S372
- Bates TR, Lynch JP (1996) Stimulation of root hair elongation in *Arabidopsis thaliana* by low phosphorus availability. *Plant Cell Environ*, in press
- Boller T, Wiemken A (1986) Dynamics of vacuolar compartmentation. *Annu Rev Plant Physiol* 37: 137–164

- Cosgrove D (1986) Biophysical control of plant cell growth. *Annu Rev Plant Physiol* 37: 377–405
- Cosgrove D (1993) Water uptake by growing cells: an assessment of the controlling roles of wall relaxation, solute uptake, and hydraulic conductance. *Int J Plant Sci* 154: 10–21
- Derksen J, Emons AM (1990) Microtubules in tip growth systems. In: Heath IB (ed) *Tip growth in plant and fungal cells*. Academic Press, San Diego, pp 147–181
- Derksen J, Rutten T, Van Amstel T, De Win A, Doris F, Steer M (1995) Regulation of pollen tube growth. *Acta Bot Neerl* 44: 93–119
- Dolan L, Duckett CM, Grierson C, Linstead P, Schneider K, Lawson E, Dean C, Poethig S, Roberts K (1994) Clonal relationships and cell patterning in the root epidermis of *Arabidopsis*. *Development* 120: 2465–2474
- Emons AM (1987) The cytoskeleton and secretory vesicles in root hairs of *Equisetum* and *Limnobia* and cytoplasmic streaming in root hairs of *Equisetum*. *Ann Bot* 60: 625–632
- Emons AMC, Traas JA (1986) Coated pits and coated vesicles on the plasma membrane of plant cells. *Eur J Cell Biol* 41: 57–64
- Galway ME, Heckman JW Jr, Hyde GJ, Fowke LC (1995) Advances in high-pressure and plunge-freeze fixation. In: Galbraith DW, Bourque DP, Bohnert HJ (eds) *Methods in cell biology*. Academic Press, San Diego, pp 3–19
- Heath, IB (1985) Evidence against a direct role for cortical actin arrays in saltatory organelle motility in hyphae of the fungus *Saprolegnia ferax*. *J Cell Sci* 91: 41–47
- Kiss JZ, Giddings TH Jr, Stachelin LA, Sack FD (1990) Comparison of the ultrastructure of conventionally fixed and high pressure frozen/freeze substituted root tips of *Nicotiana* and *Arabidopsis*. *Protoplasma* 157: 64–74
- Kushida H (1974) A new method for embedding with a low viscosity epoxy resin “Quetol 651”. *J Electron Microsc (Jpn)* 23: 197
- Ridge RW (1988) Freeze-substitution improves the ultrastructural preservation of legume root hairs. *Bot Mag Tokyo* 101: 427–441
- Ridge RW (1995) Micro-vesicles, pyriform vesicles and macro-vesicles associated with the plasma membrane in the root hairs of *Vicia hirsuta* after freeze-substitution. *J Plant Res* 108: 363–368
- Ridge RW (1996) Root hairs: cell biology and development. In: Y Waisel, A Eshel, U Kafkafi (eds) *Plant roots. The hidden half*, 2nd edn. Marcel Dekker, New York, pp 127–147
- Schiefelbein JW, Shipley A, Rowse P (1992) Calcium influx at the tip of growing root-hair cells of *Arabidopsis thaliana*. *Planta* 187: 455–459
- Schiefelbein JW, Somerville C (1990) Genetic control of root hair development in *Arabidopsis thaliana*. *Plant Cell* 2: 235–243
- Schnepf E (1986) Cellular polarity. *Annu Rev Plant Physiol* 37: 23–47
- Sherrier DJ, VandenBosch KA (1994) Secretion of cell wall polysaccharides in *Vicia* root hairs. *Plant J* 5: 185–195
- Sievers A, Schnepf E (1981) Morphogenesis and polarity of tubular cells with tip growth. In: Kiermayer O (ed) *Cytomorphogenesis in plants*. Springer, Wien, pp 265–299
- Spurr AR (1969) A low-viscosity epoxy resin embedding medium for electron microscopy. *J Ultrastruct Res* 26: 31–43
- Staebl M, Soll DR (1985) Temporal and spatial differences in cell wall expansion during bud and mycelium formation in *Candida albicans*. *J Gen Microbiol* 131: 1467–1480
- Taiz L (1984) Plant cell expansion: regulation of cell wall mechanical properties. *Annu Rev Plant Physiol* 35: 585–657
- Wiebe HH (1978) The significance of plant vacuoles. *BioScience* 28: 327–331